



**SEISMIC RISK MITIGATION
FOR THE EAST AFRICAN
COUNTRIES. CASE STUDY:
SALIMA, MALAWI**

EEFIT research grant - 2018

Dr. Viviana Iris Novelli
PRA in Earthquake Impact

Abstract

Malawi is located in the Rift area of East Africa and is classified as one of the poorest countries in the world. Scarce seismic awareness and lack of economic resources have a negative impact on the technical practice adopted to build local houses, which results in inadequate resistance against seismic loads. The poor construction techniques, together with the absence of quality control, underline an urgent need to evaluate the seismic behaviour of local buildings to make informed decisions to improve resilience through risk mitigation plans. This report presents a strategy to mitigate seismic risk with low-cost engineering solutions considering how the shortcomings of the poorly built informal masonry houses in Malawi affect their seismic response and failure modes. The proposed strategy is applied to Salima, a city in the central region of Malawi, which was severely damaged by an earthquake in 1989, causing about 50,000 homeless people. To characterize the geometric and structural characteristics of the Malawian buildings and to identify the resistance of construction materials, formal and informal settlements in Salima are surveyed, and experimental works are carried out on local masonry and typical mortars adopted in the construction practice. The acquired information is employed to derive fragility curves for the building typologies proposed for Malawi by the classification of the World Housing Encyclopaedia (Novelli et al. 2018). The effectiveness of different mitigation solutions for enhancing the seismic resilience in Salima is also discussed and evaluated by comparing the building performance before and after the retrofitting measures are applied to the existing houses. The case study shows that low-cost engineering interventions are remarkable solutions to mitigate the seismic risk in the countries of the East African Rift region.

Abstract	2
1. Introduction	4
2. Methodology	6
3. On-site data collection	7
4. Building classification	10
5. Experimental campaign	11
5.1 <i>Compressive tests for bricks; mortars and prisms</i>	<i>13</i>
5.2 <i>Tensile and shear strength of interfaces</i>	<i>14</i>
5.3 <i>Panels in diagonal shear and in out of plane</i>	<i>15</i>
6. Building performance of the houses inspected on site	16
6.1 <i>Characterisation of local masonry strength</i>	<i>17</i>
6.2 <i>Failure mode proportions of the inspected buildings</i>	<i>18</i>
7. Seismic mitigation program	19
7.1 <i>Capacity curves of inspected buildings before and after retrofitting</i>	<i>22</i>
8. Fragility curves	24
9. Conclusions	27
Acknowledgement	27
References	28

1. Introduction

East Africa is exposed to different natural hazards: such as floods, tsunamis, volcanic eruptions, winds and droughts; which can potentially become catastrophic events, because of its poor rural livelihoods. In these regions, the seismicity is ranked as moderate, although past earthquakes have recorded several damage and losses along the East African Rift System (EARS), the largest continental seismic rift system on earth. Currently, in the Rift System there are more than 30 million of poor urban households, number which might increase to 60 million by 2050 due to the rapid urbanization and population growth in these regions (Saghir and Santoro; 2018), therefore the impact of future events is likely to be more severe.

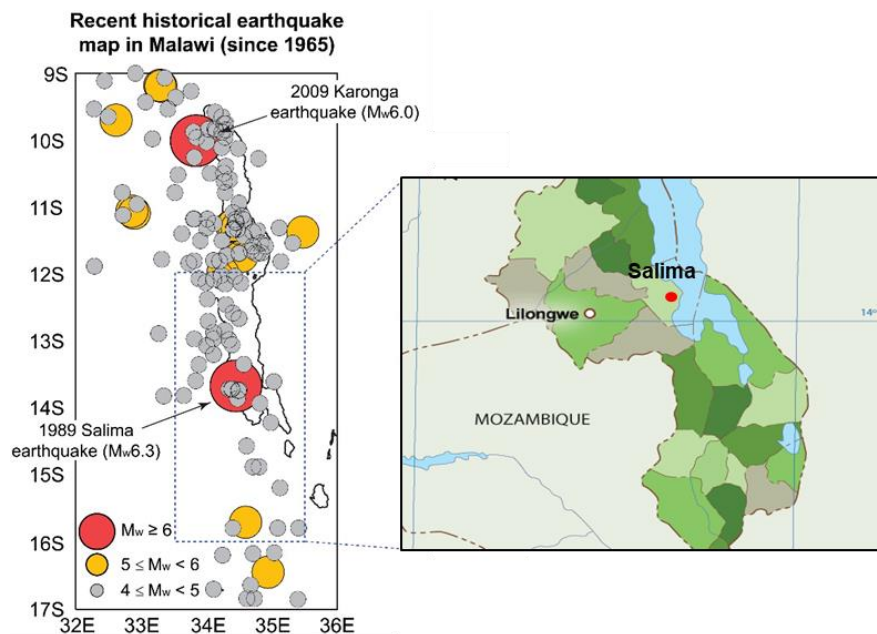


Figure 1: Recent historical earthquake map in Malawi, and identification of the township Salima,

Malawi is located within the western branch of the East African Rift System and is one of the least developed countries around the world. Malawi is exposed and vulnerable to negative economic impacts of natural disasters (e.g. drought, heavy rains, windstorms, floods and earthquakes). Agriculture, the primary economic activity of Malawi, generates around 80 percent of total export earnings and employment. As a result of climate change, the intensity, duration, and frequency of weather-related shocks have a key role in the economic cycle, with negative impacts of bad weather compounded by factors such as

population growth and environmental degradation. (FAO- IFAD-WFP, 2015; World Bank, 2017).

In Malawi, see Figure 1, seismic risk is not negligible because earthquakes of Mw7+ occurred in the past (e.g. 1910 Rukwa Tanzania and 2006 Mozambique earthquakes, Hodge et al. 2015, Poggi et al. 2017). In the last few decades, Malawi experienced several moderate (Mw6+) events, such as the 1989 Salima earthquake (Gupta and Malomo, 1995) and the 2009 Karonga earthquake (Biggs et al., 2010), which caused significant damage to non-engineered constructions, built by local artisans with little input from qualified engineers. Currently, the official code of practice for masonry construction is MS791-1:2014 (Malawi Bureau of Standards, 2014). This code is based on the British Standard and is not usually complied with. The specified practice in the code requires high construction skills and extensive economic resources. For informal settlements, the Safer Housing Construction Guidelines (Bureau TNM, 2016) have been developed to provide guidance on good practice to construct low-cost masonry buildings. Although the Guidelines are a significant source of information to understand how buildings in informal settlements should be built, communities do not always opt for such solutions because they are not usually affordable. Furthermore, since a dissemination plan of the existing guidelines is not in place, house owners and local builders are often unaware of these guidelines, which are currently only available in a digital format.

This report aims to evaluate the seismic vulnerability of non-engineered constructions in Salima, selected as a representative township in the central region of Malawi, because of its rapid urban growth and construction practice. Based on data collected on site for 113 buildings, seismic performance of existing houses was evaluated by using a viable mechanical approach, FaMIVE (Failure Mechanism Identification and Vulnerability Evaluation; D'Ayala and Speranza, 2003; D'Ayala, 2005; Novelli et al., 2015). FaMIVE can evaluate failure mode proportions, cumulative damage and capacity and fragility curves of buildings on the basis of geometrical/structural features observed on site and mechanical parameters derived experimentally. For the inspected buildings, retrofitting interventions are proposed according to the predicted failure modes and derived cumulative damage curves, and they are recommended as solutions to improve seismic building performance and actual building practice in the country. The effectiveness of the proposed low-cost engineering interventions is also discussed by comparing fragility curves assessed before and after retrofitting interventions. Results provide useful data for the development of structural vulnerability evaluation tools for masonry structures in Malawi, and for the

implementation of risk assessment frameworks for East African countries (Goda et al., 2018).

2. Methodology

The methodology is outlined in Figure 2. Brief descriptions of each phase of the procedure are:

- On-site data collection
Buildings are described with reference to their geometrical and structural features observed through on-site structural surveys, carried out in May 2018. Collected information is statistically analysed to define parameters and their variability quantitatively, which most impact the seismic performance of non-engineered masonry buildings.
- Building classification
Buildings are classified within the non-engineered masonry building classifications presented by the authors in the World Housing Encyclopedia (Novelli et al., 2018). Three different typologies are introduced with reference to the parameters observed on site with the scope at defining the vulnerability characterising the identified classes.

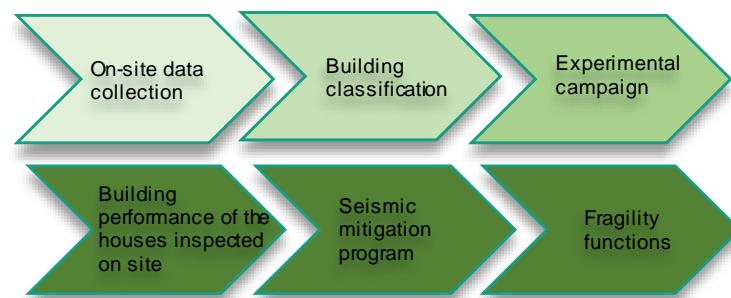


Figure 2: Methodology. (Adapted from Novelli et al. 2019-a, 2019-c).

- Experimental campaign
Strength of local materials are defined following the experimental campaign performed in September 2018 (Kloukinas et al., 2019). Results are adopted to characterise mechanical properties of bricks and mortar ad to assess the failure modes of panels tested in shear and in flexure.

- *Building performance of the houses inspected on site*
Characterised mechanical properties and strength of construction materials, and known the geometric and structural features of buildings, FaMIVE (D'Ayala and Speranza, 2003; D'Ayala, 2005; Novelli et al., 2015), based on a mechanical approach, is adopted to derive load factor multipliers, which estimate the maximum lateral acceleration (%g) triggering the failure modes which have the highest possibility of occurrence and cause the collapse of the inspected buildings.
- *Seismic mitigation program*
Observed deficiencies and estimated failure mode proportions for the inspected buildings are estimated to identify suitable low-cost engineering solutions for preventing the failure modes that have the highest possibility of occurrence. In order to validate the effectiveness of the recommended low-cost engineering solutions, cumulative damage curves and capacity curves are derived before and after the proposed retrofitting strategies (D'Ayala and Speranza, 2003; D'Ayala, 2005; Novelli et al., 2015).
- *Fragility curves*
To assess the probability of collapsed buildings for difemerine spectral acceleration values, fragility functions are derived for building typologies before and after the recommended retrofitting solutions (D'Ayala and Speranza, 2003; D'Ayala, 2005; Novelli et al., 2015).

3. On-site data collection

On-site structural surveys were carried out on 113 non-engineered buildings located in formal and informal settlements in the urban areas of Salima (see Figure 1). For each building, data were collected only for two orthogonal façades, since parallel walls of the inspected buildings had similar opening layouts. Data collection consisted of taking geometrical measurements (e.g. plan geometry, building/gable height, and opening dimensions and layout). Information related to structural features of the inspected houses, such as masonry and mortar type and roof structure type, was also collected. Furthermore, since the inspected houses were constructed using locally sourced materials with poor quality control, and construction materials differ considerably in shape, homogeneity,

consistency, density, and brittleness, the quality of the observed construction materials was recorded and defined as:

1. good fabric quality (see Figure 3a): bricks have regular shapes and mortar layers. The clay, from which the bricks were made, has a homogeneous texture. Brick bonding is regular. The bricks might have hair-line cracks or cracks are apparently absent (Novelli et al. 2019-b, 2019-c).
2. medium fabric quality (see Figure 3b): bricks have partially regular shapes and mortar layers. The clay, from which the bricks were made, has a medium porosity. Brick bonding is partially regular. The bricks might have light cracks or small holes (Novelli et al. 2019-b, 2019-c).
3. poor fabric quality (see Figure 3c): bricks have irregular shapes and mortar layers. The clay, from which the bricks were made, has high porosity. Overlapping of bricks is irregular. The bricks have deep cracks or are partially lost (Novelli et al. 2019-b, 2019-c).



Figure 3: a) Good fabric quality; b) medium fabric quality; c) poor fabric quality; (Adapted from Novelli et al. 2019-c).

In Table 1, the inspected buildings are classified according to roof type (thatched/metallic sheet), mortar type (mud/cement), fabric quality (1: good, 2: medium; 3: poor) and quality of connections between the walls (good/poor). Photographs of the main features related to fabric quality, connections between walls, mortar types and roof structures of the inspected constructions are illustrated in Figure 4(a) to Figure 4(f).

The inspected houses in Salima were made of fired bricks, most affordable material for the country, since it is sourced on-site, and requires low construction skills to be produced locally. Sun-dried bricks observed elsewhere in Malawi (Novelli et al., 2018), do not appear to be still used in Salima. Mud mortar was identified for 58% of the inspected buildings, while cement mortar, observed for the remaining inspected houses, is gradually being adopted. Fabric quality varies considerably from poor to good and underlines the need of

assessing the building performance by defining mechanical properties which reflect the actual masonry strength according to the different fabric quality levels identified on site.

Table 1. Building proportions with reference to the main features affecting the seismic building performance (i.e. roof, masonry, mortar and connection types, fabric quality (for the latest; 1: good; 2: medium and 3: poor)). (Adapted from Novelli et al 2019-c).

Total number of inspected buildings = 113

Roof type	Thatched roof		Metallic sheet roof				
Masonry type	Fired bricks						
Mortar type	Mud		Mud			Cement	
Fabric quality	2	3	1	2	3	1	2
Poor connections	8%	4%	3%	24%	4%	1%	4%
Good connections	1%	0%	2%	13%	0%	20%	18%



Figure 4: a) poor connection at the bottom of walls; b) local masonry made of fired brick with cement mortar; c) local masonry made of fired brick with mud mortar; d) complete disconnections between adjacent walls due to poor connection e) thatched roof; and f) metallic sheet roof. (Adapted from Novelli et al 2019-c).

42% of the inspected houses were built with single-skin walls with thickness varying from 100 mm to 160 mm. For these structures, the connections between adjacent walls were assumed poor, while for the remaining inspected houses with double-skin walls and thickness varying from 210 mm to 260 mm, the connections between walls were assumed stronger only if cement mortar was employed. According to the on-site observations, 53% of the inspected houses were deemed to have good quality of the connections. Regarding building roofs, these were made of timber rafters supporting thatch for 13% of the inspected buildings or light metallic corrugated sheets for the remaining ones. Both roof types were

inspected on site and classified as light systems, as they are not rigid and therefore undergo deformations in their own plane and do not act as a rigid diaphragm.

4. Building classification

According to the collected data described above, the inspected buildings are classified in three typologies: A, B, and C (shown in see Figure 5), with reference to the classification included in the World Housing Encyclopedia (Novelli et al., 2018). The descriptions of each typology are reported as follows.

Buildings with by high seismic vulnerability are classified in typology A. This class is representative of 8% of the inspected buildings (see Figure 5 (a)). These buildings were made with fired bricks of poor fabric quality (see Figure 3(a)) bonded with mud mortar. These houses had a smaller building footprint than the typical floor plan of 8 m × 6 m. These houses had thatched roof or corrugated metallic sheets supported by light timber elements of section 100 mm x 50 mm. Constructional detailing (e.g. interlocking between bearing walls and between those and roof systems) were poorly made and lack of ordinary maintenance was evidently the major cause of the deterioration, resulting in loss of bricks, severe cracks on walls and rot in timber elements adopted for roofs and opening frames.



Figure 5: Typical masonry buildings in Malawi; a) typology A; b) typology B; and c) typology C. (Adapted from Novelli et al. 2019-c).

The most common typology observed in Salima is B, class defined to characterise uses with medium seismic vulnerability. This typology covers 50% of the inspected buildings, (see Figure 5(b)). These buildings were made of fired bricks with a quality fabric which varied from medium to good (Figure 3(b) and Figure 3(c)). The type of mortar adopted for these houses was mud, therefore the bonding between bricks and connections between walls were highly weak. These houses had a typical floor plan of 8 m × 6 m. The construction details varied significantly as well as the maintenance levels.

Buildings in typology C have a low seismic vulnerability. This class covers 42% of the inspected houses, (see Figure 5(c)). These were made of fired bricks with a quality fabric varying from medium to good (Figure 3(b) and Figure 3(c)). The mortar adopted to bond bricks was cement. These houses had a larger building footprint than the typical floor plan of $8\text{ m} \times 6\text{ m}$. Due to the extended plan size, irregularities in plan were likely to occur (e.g. portico and re-entrant corner). Most of these houses had corrugated metallic sheets supported by timber elements or trusses, and good structural detailing (e.g. adjacent walls and walls/roof are well connected). The good structural quality of these houses can be also attributed to the presence of strengthening elements (e.g. ring beams).

5. Experimental campaign

Mechanical properties of masonry materials commonly used for housing in Malawi were investigated by means of laboratory testing designed with the aim at a) replicating the actual construction practices observed in Salima and b) characterising strength of local materials in the country (Kloukinas et al., 2019).



Figure 6: Masonry adopted for the specimens.

The experimental tests were jointly designed by The Polytechnic (Blantyre, Malawi) and the University of Bristol (Bristol, UK), and were carried out at the Civil Engineering Laboratory at the Polytechnic. Test configurations consisted of:

- 1) Compressive tests on a) fired bricks, b) mud mortar samples, c) cement mortar samples made with different sand ratio and d) prisms. These tests aimed at characterising the vertical strength of the most common material adopted in the country.

- 2) Tensile and shear tests on couplets and triplets. These tests were performed to measure the quality of bonding between mortar and bricks in terms of strength; cohesion and friction.
- 3) Diagonal shear test and out of plane tests on panels. These tests are carried out to assess strength and behaviour of wall panels subjected to different types of loading, and to identify possible failure modes dominating a panel collapse.

At least 6 specimens were prepared for each of different test. Specimens were built using local commercially produced bricks with nominal dimensions of 200mm × 90mm × 50mm. Those bricks, although they were from the same batch, exhibited a large variation in the fabric quality (i.e. colour, shape, and size, as illustrated in Figure 6).

Two types of mortars were investigated: 1) mud, mostly adopted material for houses with single/double skin walls characterised by a fabric quality varying from poor to medium and 2) cement, mostly adopted material for houses with double skin walls characterised by a fabric quality varying from medium to good. In addition to this, for the cement mortar, different cement-to-sand mixtures were employed: 1:4; 1:6 and 1:8, where the first two are the values recommended by the MS791-1 (Malawi Bureau of Standards, 2014) and the Safer House Construction Guidelines (Bureau TNM, 2016), respectively, while the last one is the cement-sand ratio which is mostly affordable; and therefore mostly adopted by local artisans.



Figure 7: Typical testing configurations.

The cement mortars adopted for prisms and panels were prepared in two conditions: a) “Unfavourable” by applying mortar on dry and dusty bricks and b) “Favourable” with bricks soaked in water prior to masonry construction. Hereafter, a letter “F” or “U” is added to the mortar type to indicate the simulated bonding conditions, e.g. 1:4F.

The equipment used for the experiments consisted of a combination of some testing rigs mountable on the specimens directly, a laboratory's strong floor, and a high-precision video tracking system for measurement of displacements, and synchronised analogue load cell signals connected onto it for measurement of maximum strengths. Some typical photos of the basic testing configurations are shown in Figure 7.

5.1 Compressive tests for bricks; mortars and prisms

The compressive tests on bricks were performed according to MS6, 1994; MS777, 1997; and EN 1015-11, 1999, as illustrated in Figure 8a. The test was carried out for a few bricks corresponding to 1% of the total batch employed to build all specimens. Figure 8b shows the typical failure mode observed during the compressive tests on bricks.

The results highlight a significant scatter in the values measured to characterise the mechanical properties of the tested masonry: compressive strength varies from 2MPa to 10 MPa (Kloukinas et al., 2019). Since compressive strength depends on the fabric quality, and the masonry adopted in the test was significantly characterised by irregular shapes and colours; the scatter measured in the strength for the tested bricks was an expected result.

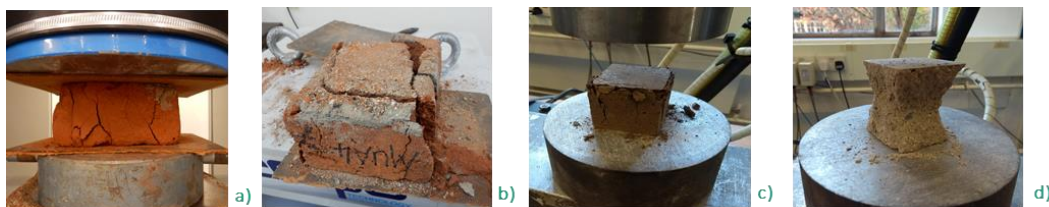


Figure 8: a) and c) Compressive test on bricks and mortar samples and b) and d) related failure modes.

The test on mortar were performed on 50mm mortar cubes, as the ones illustrated in Figure 8c. Three sets of samples were employed: 1) mud, 2) cured cement in water for 28 days and 3) air-dried cement. Figure 8d shows the typical failure mode observed during the compressive tests on mortar samples. The test on the mortar exposes a compressive strength of 2 MPa for mud cubes, and a reduction of compressive strength for cubes with a smaller cement content, from 13 MPa to 4MPa for cured samples and from 6MPa to 2 MPa for air-dried samples (Kloukinas et al., 2019). The tests show not only a 50% reduction of compressive strength in the cement sample due to bad curing conditions, but also that the weakest cement mortars under bad curing conditions, proved to be as weak as the traditional mud mortar material.

The masonry prisms were made of five brick high to satisfy standard slenderness limits (EN 1052-1, 2002) and a base around 1060mm, in agreement with standard method presented by Brignola et al. (2008), as illustrated Figure 9. The values obtained for the compressive strength on prisms are lower than the ones obtained for brick units and mortar samples (e.g. values vary from 0.75MPa to 1 MPa for the weaker prisms made with mud mortar, and from 1MPa to 2MPa for strongest prisms made with cement-sand ration of 1:4, Kloukinas et al., 2019). The failure mechanism in these tests was governed by local crushing of the weakest bricks in the stack.



Figure 9: Compressive tests and related failure modes for masonry prisms; note the local brick crushing mechanism in the bottom pictures.

5.2 Tensile and shear strength of interfaces

The measurement of the tensile and the shear strength was performed on crossed couplets (ASTM C952) and triplets (EN 1052-3, 2002) made of bricks bonded with 1) mud mortar and 2) cement to sand ratio of 1:4F; and 1:8U, see Figure 10. The tests expose a median tensile resistance of the interfaces of 0.008 MPa for couplets with mud mortar. Furthermore, it is observed an expected reduction of the median tensile resistance in couplets with a smaller cement content; varying from 0.092 MPa to 0.039 MPa for 1:4F couplets and from 0.049 MPa to 0.040 MPa for 1:8U couplets (Kloukinas et al., 2019).



Figure 10: Compressive tests and related failure modes for masonry prisms; note the local brick crushing mechanism in the bottom pictures.

The increment of strength in the interface due to a high cement content in the mortar and a favourable bonding conditions is also observed during the tests performed on triplets. Using the Mohr-Coulomb shear failure criterion parameters; interface cohesion is between 0.01 and 0.02 MPa for triplets with mud mortar to 0.15-0.25 MPa for triplets with the strongest cement mortar configurations (1:4F). Friction angles were measured at around 32 degrees (Kloukinas et al., 2019).

5.3 Panels in diagonal shear and in out of plane

Diagonal shear tests were performed on square panel five brick unit long (or around 1060mm), according to the standard method, presented by Brignola et al. (2008). Panels were made only using a cement-sand ratio of 1:6U and 1:4F, see Figure 11. The differences in strength and stiffness are obvious for the different configurations. During the test, the premature failure of many specimens corresponded to parallel sliding along a “weak” joint, rather than a diagonal crack. The results exposed a maximum shear stress varying from 0.2 MPa to 0.3 MPa and from 0.05 MPa to 0.1 for panel with cement-sand ratio of 1:6U, for panel with cement-sand ratio of 1:4F, respectively (Kloukinas et al., 2019).

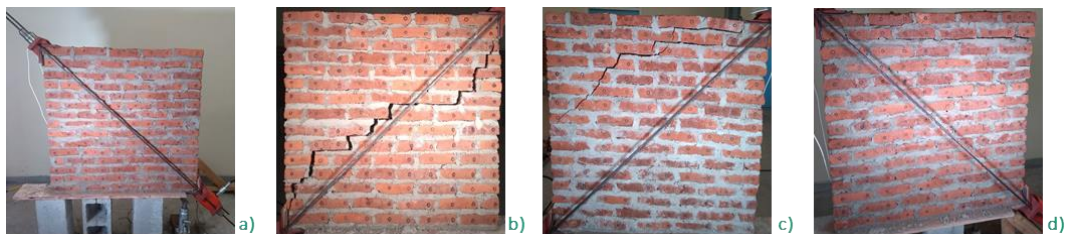


Figure 11: a) Typical setting for diagonal shear test on square panels. b) failure mode along the weak bed joint c) failure mode along the weak bed joint and weak bricks d) failure mode along the weak bed joint associated to a “dry” joint.

The out-of-plane flexure test on panels were performed along two different axes, parallel and perpendicular to the brick bending (EN 1052-2, 2002, MS791-1, 2014). In both cases, the span of the supports for the bending beam was 800 mm, to satisfy standard length to thickness limits (MS791-1, 2014). Panels were made using only cement mortar with a cement-sand ratio of 1:6U 1:4F, see Figure 12. The value of the mean flexure strength (~0.05 MPa) measured parallel to the brick bending has similar values for the various panels made with different cement sand ratio of 1:4F and 1:6U (Kloukinas et al., 2019). This was observed because quality of the interface bonding governs the behaviour, causing cracks in the middle span of the bending beam, i.e. the location of maximum bending

moment. On the other hand, it was observed that the flexure strength in the perpendicular to the brick bending test had a notable different value for panels with cement sand ratio of 1:4F made and 1:6U (i.e. 0.5 MPa and 0.3 MPa, respectively (Kloukinas et al., 2019)). The weaker 1:6U panels failed due to parallel sliding of the bricks on the interfaces, with the bricks left intact, whereas the stronger 1:4F failed with a vertical crack passing through vertical mortar joints and bricks (Kloukinas et al., 2019).



Figure 12: Out-of-plane flexural failure modes: (a) parallel and (b) perpendicular to the brick bending.

6. Building performance of the houses inspected on site

The seismic performance of the identified typologies in Section 4 was estimated using FaMIVE (D'Ayala and Speranza, 2003; D'Ayala, 2005; Casapulla and D'Ayala, 2006; Novelli et al., 2015). The approach is based on a mechanical procedure, relying on the assumption that buildings behave as an assemblage of macro-elements, held together by compressive forces. Analyses were performed using equilibrium equations, where earthquake actions are simulated as a horizontal static force, proportional to the mass of the single inspected façade. The analysis aimed at predicting the horizontal static actions (maximum lateral accelerations), quantified by means of collapse load factor multipliers (λ) (D'Ayala and Speranza, 2003; D'Ayala, 2005; Novelli and D'Ayala, 2012). The factor λ was calculated for each of the failure modes, which are defined as all possible collapse mechanisms that can occur for a masonry building subjected to earthquake shaking. The estimated values of λ indicate the lower bounds of the level of shaking which trigger the identified failure modes. Among the computed collapse load factor multipliers, the failure mode with the smallest multiplier is considered to occur on a façade (as the weakest link). In implementing FaMIVE method, the geometrical/structural features collected on site and described in Section 3 were adopted to characterise the building typologies identified in

Section 4. Mechanical properties of the identified typologies were defined with reference to the test discussed Section 5 with reference to the assumption described in section 6.1.

6.1 Characterisation of local masonry strength

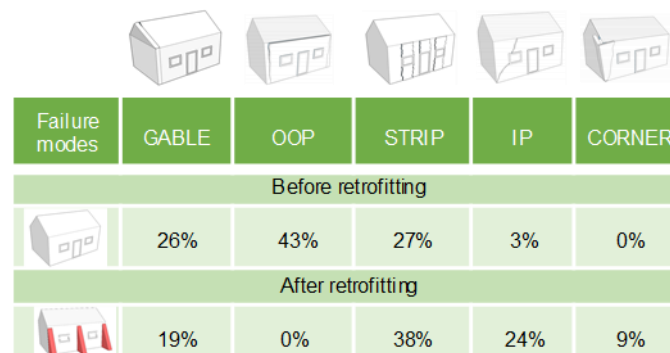
To be consistent with the data collected on site, see section 3, and with the poor brick-mortar bonding measured in the tested couplets and triplets made with fired bricks and mud mortar, see Section 5.2, the connections between single skin/double walls for buildings in typology A and typology B were assumed absent. Furthermore, to take into account that for the inspected buildings in Salima, as confirmed by local artisans, bricks were made under bad curing conditions, see Section 5, only tested samples made in unfavourable condition are used to characterise the mechanical properties of local materials. The only expectations were made for buildings in typology C with fired bricks of a good fabric quality, where it was assumed that bricks were soaked in water prior to construction. Therefore, for these buildings the cement-sand ratio was assumed 1:6F (in agreement with the recommendations of the guidelines) while for all other buildings in typology C, cement-sand ratio was assumed 1:8U; which is mostly affordable and adopted by local artisans, see Section 5 for the definition of F and U.

To characterise brick-mortar bonding of the typologies A, B and C, introduced in section 4, interface cohesions and friction angle were defined with the reference to the values measured during the test. The adopted values are:

- for buildings with mud mortar in typology A and B, the interface cohesion varies from 0.01 (from poor fabric quality of bricks) to 0.02 MPa (to good fabric quality of bricks).
- for buildings with the strongest cement mortar (1:6F) in typology C, the interface varies from 0.06 (poor fabric quality bricks) to 0.12 (good fabric quality bricks) MPa.
- for buildings with the poorest cement mortar (1:8U) in typology C, the interface varies from 0.04 (poor fabric quality bricks) to 0.08 (good fabric quality bricks) MPa.
- friction angles were measured at around 32 degrees (Kloukinas et al., 2019).

6.2 Failure mode proportions of the inspected buildings

Failure modes associated with the identified collapse load factor multipliers derived from FaMIVE are illustrated in Figure 13. These are classified into five categories: 1) *GABLE*: predominantly occurs on walls with gables which are not connected to roofs, and therefore fail in overturning; 2) *OOP* (out-of-plane): predominantly occurs on single-skin walls with poor-quality materials and poor connections between walls and between walls and the roof, causing overturning of a single façade; 3) *STRIP*: predominantly occurs on single-/double-skin walls with medium quality materials and good connections between walls and between walls and the roof, causing overturning of vertical strips of piers or spandrels; 4) *IP* (in-plane): predominantly occurs on single/double-skin walls with medium to good quality materials and good quality connections between walls and between walls and the roof, causing shear failure of a single façade 5) *CORNER* (corner failure): predominantly occurs on buildings with good quality materials and good quality connections between walls and between walls and the roof, causing overturning of at least two orthogonal adjacent façades.



Failure modes	GABLE	OOP	STRIP	IP	CORNER
Before retrofitting					
	26%	43%	27%	3%	0%
After retrofitting					
	19%	0%	38%	24%	9%

Figure 13: Failure mode proportions for the inspected building sample in Salima before and after the retrofitting plan proposed in Section 6.2. (Adapted from Novelli et al. 2019-c).

As expected from the on-site surveys, since a lack of connections between the walls and roof and poor quality construction materials were frequently observed in the inspected buildings (see Table 1), *OOP* is the most likely failure mode with a percentage of 43%, followed by *STRIP* (27%), then *GABLE* (26%). Only 3% of the inspected houses are expected to fail *IP*, and *CORNER* is not the identified failure mechanism for any of the investigated buildings. The results highlight that even buildings of typology C, built with double-skin walls, fired bricks with a good fabric quality, are expected to fail mostly due to overturning of gables, walls, spandrels and piers.

7. Seismic mitigation program

Several types of interventions based on low-cost engineering solutions can be suggested to improve the structural performance of the inspected non-engineered masonry buildings in Salima (Novelli et al. 2019a). Descriptions of recommended retrofitting interventions include:

- Wall plates (see Figure 14a, and b).

These elements are made as horizontal timber bands installed along the tops of walls under the roof to provide a fixing point at the ends of the rafters and to ensure connection between the tops of walls and the roof. These elements are fixed to walls through steel or timber pegs. In the inspected houses in Salima these elements were rarely used under the rafters, which generally seated directly on top of walls, which often resulted in severe local damage to the walls by the rafters due to stress concentration. To prevent high stress concentration at rafter-wall contact points and to improve connections between walls and the roof structure, wall plates are highly recommended.

- Ring beams (see Figure 14c).

Ring beams (also known as a crown, collar, band or tie beams or seismic beams) are made of reinforced concrete or timber and are located as a belt at roof and/or lintel level. These elements are used to ensure that gravitational/seismic loads are properly transferred, and connections on top of walls prevent out-of-plane failure modes. In this respect, in the Safer Housing Construction Guidelines (Bureau TNM, 2016), there is a specific section for ring beams, where it is advised to combine ring beams at lintel and roof levels as only one beam, which should be located at roof level.



Figure 14: a) Timber wall plate of rectangular section, b) timber wall plate of circular section, and c) concrete ring beam. (Novelli et al. 2019-a).

This has been suggested to reduce complexity and cost in the building process. In practice, as discussed in Section 3.2, concrete ring beams are rarely used, and they are only placed at lintel level, supporting spandrels, which can be highly vulnerable under earthquakes, if they are deep in height. The observed ring beams were often under-designed to support gravitational/seismic loads and since they were not connected directly to roofs, these were not capable of constraining roof structures. Existing ring beams need to be inspected and substituted with new ones, if they are deficient. Furthermore, it is strongly advised that ring beams be placed both at lintel and roof levels, or only at the lintel level, if spandrels are not significantly deep in height. Use of ring beams at roof level only should be considered, if lintels on the top of openings are also adopted.

- Buttresses (Figure 15a)

The failure mode that has the highest possibility of occurrence in buildings made of masonry with poor fabric quality and lack of connections between walls and the roof, is *OOP*. This was confirmed by the results obtained in Section 6.1, as well as by many of the recent post-earthquake assessments performed on unreinforced masonry constructions (Wilkinson et al., 2011; Ioannou et al. 2012; Novelli and D'Ayala, 2012; Kaushik et al., 2016).

In order to prevent this failure mode, in this section the use of buttresses is proposed as a low-cost engineering solution to enhance the seismic resilience of the Malawian houses. An example of buttresses can be found in Figure 15a. These structural elements could be constructed using fired bricks and cement or mud mortar and should be located perpendicular to walls which are vulnerable to fail in overturning under seismic loads. Buttresses have not only the function to prevent out-of-plane failure modes, but also to increase stability of buildings, reducing the structural period (Ortega et al., 2018).

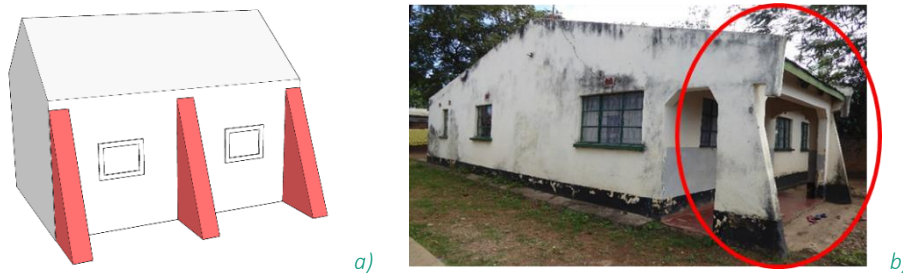


Figure 15: a) Buttresses: structures made of stones or bricks, built against walls, to prevent overturning b) buttresses observed on-site during structural surveys. (Novelli et al. 2019-a).

In Salima, buttresses are elements built in new houses made of fired bricks and cement mortar, and are used on the outside of the houses, to create a space which is not exposed to sun. These elements are generally located on the longest wall of the front side. Commonly, only two buttresses are built, one is generally located on the edge of the wall while the second one is on the centre of the wall. In order to prevent building to fail for torsion under seismic events, it is recommended to ensure that buttresses are well connected to the entire houses and located symmetrically respect to the house plan.

The effectiveness of buttresses to improve seismic building performance is presented in Figure 12, where the use of these elements significantly favours the occurrence of *IP* failure modes, which occur for 24% of the inspected façades, and fully prevents *OOP* successfully. The number of buildings failing for the out of plane of *GABLE* is decreased, increasing the proportion of buildings failing for *STRIP*. This underlines that the use of buttresses is a suitable mitigation solution to prevent overturning of the entire walls but do not enhance the strength of single piers and spandrels, depending on the fabric quality and the interface between masonry and mortar. This underlines that if buildings are built with poor materials and poor fabric quality and connection between walls are strengthened using buttresses, the failure modes with the highest probability of occurrence becomes the overturning of a strip of pier or a strip of spandrels. Therefore, only increasing cement in the mortar, masonry with good fabric quality, and favourable bonding conditions, as observed during the test, houses will have higher strength and therefore fail in *CORNER*. This is also emphasised by the small number of buildings failing in *CORNER* modes (9%), which occur only in buildings of typology C made of double skin walls of fired bricks characterised by a good fabric quality and mortar with a cement-sand ratio of 1:6F.

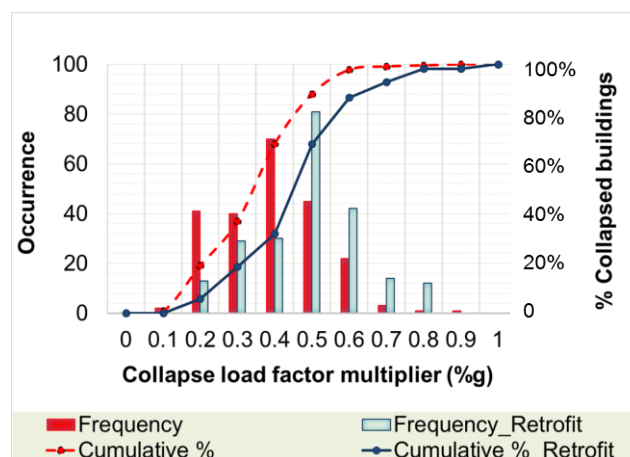


Figure 16: Occurrence of the identified collapse load factor multipliers and cumulative damage curves for the inspected building sample in Salima before and after the retrofitting plan proposed in Section 6.2. (Adapted from Novelli et al. 2019-c).

The impact of the buttresses is also underlined by the cumulative damage curves shown in Figure 16, where the median of λ before and after retrofitting is increased from 0.34g to 0.47g. Furthermore, the initial slope of the cumulative damage curve is changed: the one derived for buildings before retrofitting has a steeper initial slope than the one derived after retrofitting (e.g. for $\lambda = 0.30g$, the percentages of collapsed buildings are 40% and 20% before and after retrofitting, respectively).

7.1 Capacity curves of inspected buildings before and after retrofitting

In this section, capacity curves are derived for the building typologies identified in Salima with reference to the methods outlined in D'Ayala and Speranza (2003), D'Ayala (2005), Casapulla and D'Ayala (2006) and Novelli et al. (2015). Derived capacities strictly correspond to the parameters of the inspected buildings in the case study (i.e. geometry, structural conditions, connection level between walls, material types, and fabric quality). Multiple capacity curves, one for each analysed façade, are derived for a single inspected façade. This is because capacity curves are directly developed from the load factor multipliers, which are also calculated for each inspected façade, as illustrated in Section 6.2.

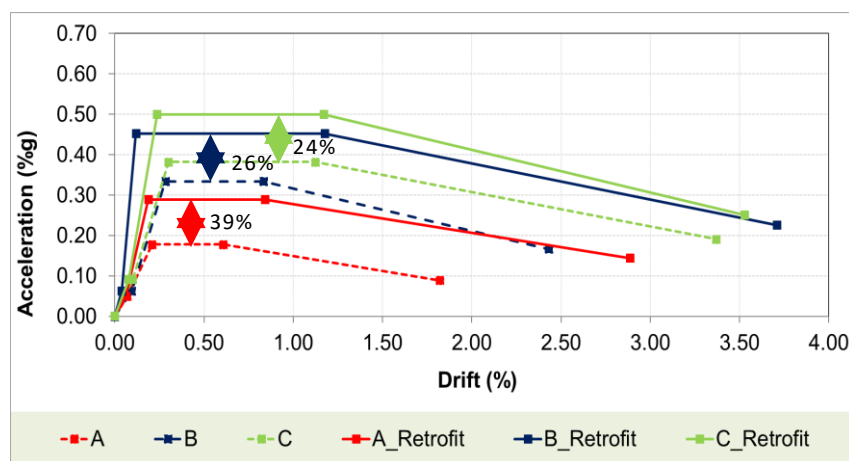


Figure 17: Capacity curves for a) typologies A, B and C; and b) failure mode classes (GABLE, STRIP, IP, OOP, and CORNER) for the inspected building sample in Salima before and after the retrofitting plan proposed in Section 6.2. (Adapted from Novelli et al. 2019-c).

The maximum strength or maximum acceleration (%g) in a capacity curve is taken equal to the minimum collapse load factor estimated by FaMIVE for each inspected façade. The elastic limit displacement of each façade is calculated as a function of the elastic stiffness

and the mass of the façade involved in the identified failure mode. The ultimate displacement is defined as the displacement identifying the geometrical instability of the façade and hence its collapse. After computing these displacements, they are divided by the height of the single inspected façade to derive the drift ratio.

Figure 17 shows different capacity curves derived for the building typologies A, B, and C identified in Salima before and after the retrofitting plan proposed in Section 6.2. As expected from the definition of the three typologies, it is noticeable that the building typology A (typology of buildings characterised by low quality materials and construction details) has the lowest values of maximum acceleration and drift compared to B and C. Regarding the positive influence of the buttresses, this is mainly highlighted by the increment of acceleration in all identified building typologies (increment of 39% in A, 26% in B, and 24% in C).

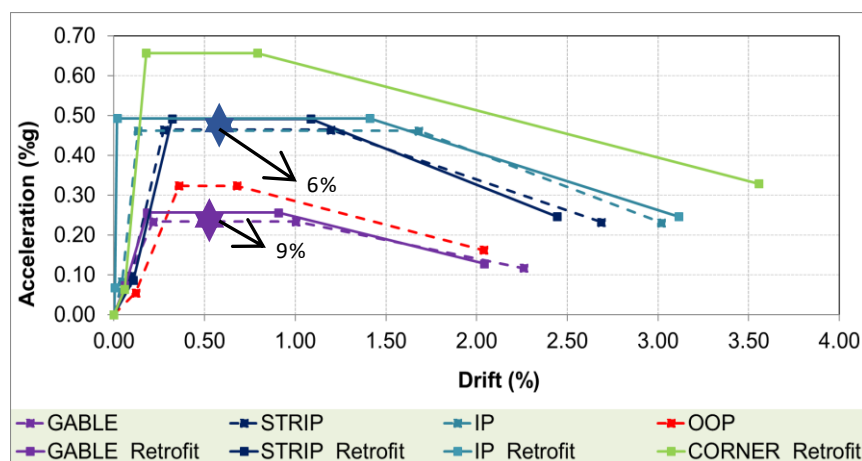


Figure 18: Capacity curves for a) typologies A, B and C; and b) failure mode classes (GABLE, STRIP, IP, OOP, and CORNER) for the inspected building sample in Salima before and after the retrofitting plan proposed in Section 6.2. (Adapted from Novelli et al. 2019-c).

Capacity curves are also derived for failure mode classes, as illustrated in Figure 18. The curves confirm that weaker buildings in topology A and B fail in *GABLE* and *OOP* modes, since they have the lowest values of structural capacity compared to the other failure modes. The presence of buttresses increases the capacity of buildings failing in the *GABLE* mode (increment of 9% before and after retrofitting), while *OOP* is prevented, as already identified in Figure 13. *IP* and *STRIP* modes are triggered by the same maximum acceleration value and occur for buildings of typology B made of good fabric quality. The presence of buttresses improves the capacities of these failure modes by 6%. This confirms

that the chosen retrofitting solution, aiming at preventing overturning of facades, positively increases the proportion of buildings failing in *IP* and *STRIP* (see Figure 13). In contrast, when buttresses are introduced in buildings with mud mortar, their presence provides only a small increment in the capacity of the single failure mode class, due to the poor bonding in the masonry. This is particularly underlined by the high capacity of *CORNER*, failure modes which occur only in buildings built with good brick fabric quality and 1:6Fcement-sand mortar.

8. Fragility curves

A fragility curve is the statistical tool to express the probability of exceeding a given damage state (e.g. collapse) as a function of an engineering demand parameter that represents the ground motion (e.g. spectral acceleration, spectral displacement, pga). In this section, fragility curves are provided by the estimated spectral acceleration SA , calculated as a function of the ultimate lateral accelerations (λ_j), load factor multipliers computed for the inspected façades in Salima to identify failure modes and corresponding capacity curves (see section 6 and 7).

SA , with reference to N2 method, is expressed by the lognormal distribution of the natural logarithms of the mean and standard deviation values of the variable λ_j by the following equations:

$$SA = e^{\bar{\mu}} \quad \text{with} \quad \bar{\mu} = \frac{1}{n} \sum_j \ln \lambda_j \quad (1)$$

$$\beta = e^{\bar{\mu} + \frac{1}{2}\sigma^2} \sqrt{e^{\sigma^2} - 1} \quad \text{with} \quad \sigma = \sqrt{\frac{\sum (\ln \lambda_j - \ln \bar{\lambda}_j)^2}{n}} \quad (2)$$

The fragility curves in Figure 19, obtained using the equations 1) and 2) show the performance of the inspected buildings in Salima, classified according to the typologies A, B and C, introduced in section 4. As expected, buildings of typology A, made of fired bricks with single skin walls are the weakest structures (e.g. for $SA = 0.20 \text{ m/s}^2$ and 0.30 m/s^2 ; the percentage of collapsed buildings is 52 and 59, respectively; against 35 and 43 obtained for

buildings of typology C, made of fired bricks with single or double skin walls with cement mortar, see Table 2).

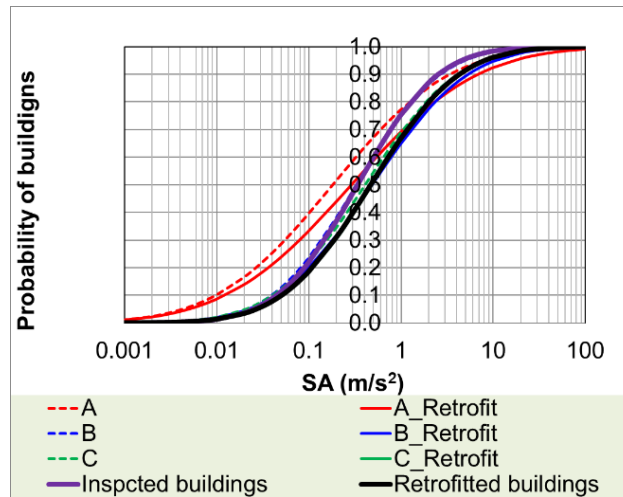


Figure 19: Comparison between fragility curves derived before and after retrofitting for the inspected buildings classified according to building typologies identified in Section 4.

Table 2. Probability of collapsed buildings, classified with reference to building typologies identified in Section 4, for the Spectral Accelerations (SA) of values 0.2 m/s² and 0.3 m/s²

		Probability of collapsed buildings						
SA	Inspected buildings	Retrofitted buildings	A	A Retrofit	B	B Retrofit	C	C Retrofit
m/s ²	%	%	%	%	%	%	%	%
0.2	37	31	52	44	38	31	35	31
0.3	48	40	59	50	48	40	43	40

Confirming the results discussed in section 7.1 for the capacity curves, buttresses particularly enhance the seismic response of buildings in typology A, preventing out of plane failure, collapse mechanism with the highest probability of occurrence due to the lack of connections between walls and gables of these houses (e.g. for $SA=0.20$ m/s²; the percentage of collapsed buildings of typology A is reduced from 52 to 44, see Table 2). It is also worth to note that buildings of typology C, classified as the strongest typologies, have only a slightly better performance compared to the other inspected buildings in Salima (e.g. total percentage of collapsed buildings in typology C is only 3% or 4% smaller than the ones identified for buildings of typology B before and after retrofitting, respectively, see Table 2). This is because, as discussed in Section 7.1, their seismic performance is highly dependent on the poor content of cement in the mortar adopted for these houses (e.g.

in typology C, buildings have low content of cement in the mortar mix, between 1:8 and 1:6; where the latest is the minimum recommended by the guidelines).

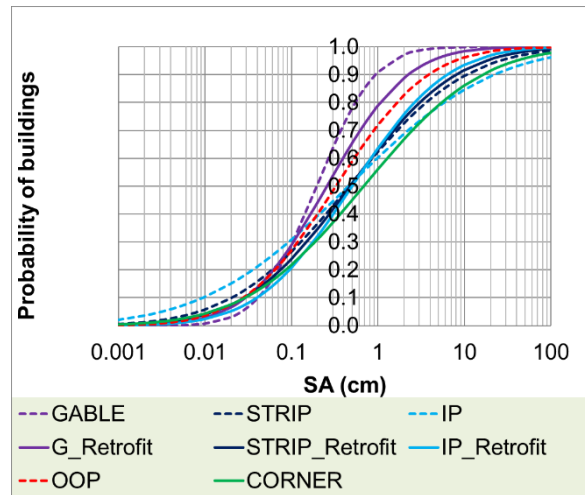


Figure 20: Comparison between fragility curves derived before and after retrofitting for the inspected buildings classified according to the failure modes identified in Section 6.2.

Table 3. Probability of collapsed buildings, classified with reference to the failure modes estimated in section 6.2, for the Spectral Accelerations (SA) of values 0.2 m/s² and 0.3 m/s².

		Probability of collapsed buildings						
SA	OOP	GABLE	GABLE Retrofit	STRIP	STRIP Retrofit	IP	IP Retrofit	CORNER
m/s ²	%	%	%	%	%	%	%	%
0.2	40	51	44	40	35	35	31	31
0.3	48	64	53	45	42	41	40	37

Fragility curves in Figure 20 are derived classifying inspected facades in Salima with reference to the failure modes estimated in Section 6.2. These functions show that percentages of collapsed buildings are notably higher for *OOP* and *GABLE*, which mainly occur for buildings in typology A, compared to *IP*, *STRIP* and *CORNER*, mainly occurring for buildings in typology B and typology C (e.g. for $SA = 0.20 \text{ m/s}^2$; the percentage of collapsed buildings is 51, 40, and 31 for *GABLE*, *OOP* and *CORNER*, respectively, see Table 3). This confirms that only a combination of a good construction practice and materials (e.g. using cement content in the mortar as recommended in the guidelines, employing bricks with a good fabric quality; constructing good connections) *GABLE*, and *OOP* can be prevented, and buildings performance for small values of *SA* can be enhanced,

favouring the occurrence of *CORNER*, which can occur even for a smaller percentage of buildings compared to the ones reported in Table 3, if these are constructed according to the recommendations provided in the guidelines and in section 7.

9. Conclusions

This report has presented a seismic mitigation plan for non-engineered masonry buildings in Malawi. The effectiveness of the proposed plan has been demonstrated by focusing on buildings located in Salima, which was selected as a representative township in the central region of Malawi for its rapid expansion of informal settlements and construction practice. The presented application on the selected area of study integrates geometrical and structural data collected on site, and mechanical properties of local materials derived experimentally, to classify building typologies and derive their performance under seismic events. Moreover, this case study demonstrates notable advantages of identifying adequate low-cost retrofitting strategies to increase seismic resilience of non-engineered masonry buildings by identifying dominant failure modes and corresponding capacity curves with and without seismic retrofitting. In the future, the framework could be further extended to a risk assessment tool and could serve to implement performance-based earthquake engineering methods for non-engineering buildings in developing countries.

Acknowledgement

The author would like to thank the many homeowners and occupants in Salima for their willingness to allow us to survey their homes. This work is supported by Earthquake Engineering Field Investigation Team research grant (2018) and the Engineering and Physical Sciences Research Council through the PREPARE project (EP/P028233/1).

References

ASTM C952, 2009. *Standard Test Method for Bond Strength of Mortar to Masonry Units*, ASTM.

ASTM C1072, 2013. *Standard Test Methods for Measurement of Masonry Flexural Bond Strength*, ASTM.

Biggs J., Nissen, E., Craig, T., Jackson, J., & Robinson, D. P. (2010). *Breaking up the hanging wall of a rift-border fault: The 2009 Karonga earthquakes, Malawi*. *Geophysical Research Letters*, 37(11).

Brignola, A., Frumento, S., Lagomarsino, S., & Podesta, S. (2008). *Identification of shear parameters of masonry panels through the in-situ diagonal compression test*. *International Journal of Architectural Heritage*, 3(1), 52-73.

Bureau TNM (2016), *Safer House Construction Guidelines*. Available at <https://issuu.com/saferconstructionguidelines/docs/no-crocini>.

Casapulla, C. and D'Ayala, D. (2006), *In-plane collapse behaviour of masonry walls with frictional resistances and openings*, 5th International Seminar on Structural Analysis of Historical Constructions, 6-8 November 2006, New Delhi, India.

D'Ayala, D. and Speranza, E. (2003), *Definition of collapse mechanisms and seismic vulnerability of historic masonry buildings*, *Earthquake Spectra*, 19(3), 479-509.

D'Ayala, D. (2005), *Force and displacement-based vulnerability assessment for traditional buildings*, *Bulletin of Earthquake Engineering*, 3(3), 235-265.

EN 1015-11. 1999. *Methods of test for mortar for masonry. Determination of flexural and compressive strength of hardened mortar*, CEN.

EN 1052, 2002. *Methods of test for masonry*, CEN.

Food and Agriculture Organization of the United Nations (FAO), *International fund for agricultural Development (IFAD)*, & *World Food Programme (WFP)* (2015), *Achieving Zero Hunger – The critical role of investments in social protection and agriculture*. Rome, FAO, 2015.

Goda, K., Kloukinas, P., De Risi R., Hodge M., Kafodya I., Ngoma, I., Biggs J., Crewe, A., Fagereng, A., and Macdonald, J. (2018), *Scenario-based seismic risk assessment for Malawi using improved information on earthquake sources and local building*

characteristics, *16th European Conference on Earthquake Engineering (16ECEE)*, 18-21 June 2018: Thessaloniki, Greece.

Gupta, H. K., & Malomo, S. (1995). *The Malawi earthquake of March 10, 1989: report of field survey*. *Seismological Research Letters*, 66, 20–27.

Hodge, M., Biggs, J., Goda, K., & Aspinall, W. P. (2015). *Assessing infrequent large earthquakes using geomorphology and geodesy in the Malawi Rift*. *Natural Hazards*, 76, 1781–1806.

Ioannou, I., Borg, R., Novelli, V., Melo, J., Alexander, D., Kongar, I., Verrucci, E., Cachill, B., and Rossetto, T. (2012), *The 29th May 2012 Emilia Romagna Earthquake–EPICentre Field Observation Report*. *EEFIT Reconnaissance Report, No. EPI-FO-290512*.

Kaushik, H., Bevington, J., Jaiswal, K., Lizundia, B., and Shrestha, S. (2016). *Buildings (EERI Earthquake Reconnaissance Team Report: M7. 8 Gorkha, Nepal Earthquake on April 25, 2015 and its Aftershocks) (pp. 5-1)*. *Earthquake Engineering Research Institute*.

Kloukinas, P., Kafodya, I., Ngoma, I., Novelli, V., Macdonald, J., and Goda, K. (2019), *Strength of materials and masonry structures in Malawi*. *SEMC 2019: The Seventh International Conference on Structural Engineering, Mechanics and Computation: 2-4 September 2019: Cape Town, South Africa*.

Malawi Bureau of Standards Board (2014), *The structural use of masonry – Code of practice, Part 1: Unreinforced masonry walling, MS791*.

Midzi, V. and Manzunzu, B. (2014), *Large recorded earthquakes in sub-Saharan Africa, Extreme Natural Hazards. Disaster Risks and Societal Implications*, 1, 214.

MS6, 1994. *Burnt bricks - specification, Malawi Bureau of Standard*.

MS777, 2007. *Stabilised Soil Blocks - Specification, Malawi Bureau of Standards*.

MS791-1, 2014. *The structural use of masonry – Code of practice, Part 1: Unreinforced masonry walling, Malawi Bureau of Standards*.

Novelli, V. and D'Ayala, D. (2012), *Assessment of the most damaged historic centres of the Region Emilia Romagna due to the earthquake of the 20th and 29th of May 2012*. *Ingegneria Sismica*, 29(2-3), 59-71.

Novelli, V.I., D'Ayala, D., Makhloufi, N., Benouar, D., and Zekagh, A. (2015), *A procedure for the identification of the seismic vulnerability at territorial scale. Application to the Casbah of Algiers*. *Bulletin of Earthquake Engineering*, 13(1), 177-202.

Novelli, V., Kloukinas, P., Ngoma, I., Kafodya, I., Macdonald, J., Goda, K. (2018), *Unreinforced masonry houses made of fired clay bricks (Report 205)*. World Housing Encyclopedia, Earthquake Engineering Research Institute, California, USA.

Novelli, V., Kloukinas, P., Ngoma, I., Kafodya, I., Macdonald, J., Goda, K. (2019-a), *Seismic Mitigation Framework for Non-engineered Masonry Buildings in Developing Countries: Application to Malawi in the East African Rift*. Book Title: *Resilient Structures and Infrastructure*, Chapter 8. DOI 10.1007/978-981-13-7446-3_8. Publisher: Springer Singapore.

Novelli, V., Kloukinas, P., De Risi, R., Kafodya, I., Ngoma, I., Macdonald, J., and Goda, K. (2019-b) *Seismic vulnerability assessment of non-engineered masonry buildings in Malawi*. COMPDYN 2019. 7th ECCOMAS Thematic Conference on Computational Methods in Structural Dynamics and Earthquake Engineering. In Crete, Greece, 24–26 June 2019.

Novelli, V., Kloukinas, P., De Risi, R., Kafodya, I., Ngoma, I., Macdonald, J., and Goda, K. (2019-c) *Seismic risk mitigation plan for countries in the East African Rift. case study: Salima, Malawi*. Society for Earthquake and Civil Engineering Dynamics (SECED) 2019. 9-10 September 2019. In Greenwich, London.

Ortega, J., Vasconcelos, G., Rodrigues, H., and Correia, M., (2018), *Assessment of the efficiency of traditional earthquake resistant techniques for vernacular architecture*, *Engineering Structures*, 173, 1-27.

Poggi, V., Durrheim, R., Tuluka, G. M., Weatherill, G., Gee, R., Pagani, M., et al. (2017). *Assessing seismic hazard of the East African Rift: A pilot study from GEM and AfricaArray*. *Bulletin of Earthquake Engineering*, 15, 4499–4529.

Saghir, J., and Santoro, J. (2018), *Urbanization in Sub-Saharan Africa Meeting Challenges by Bridging Stakeholders*. Center for Strategic and International Studies.

Wilkinson, S., Free, M., Grant, D., Boon, D., Paganoni, S., Mason, A., Williams, E., Fraser, S., and Haskell, J. (2011), *The Mw 6.3 Christchurch, New Zealand Earthquake of 22 February 2011. A Field Report by Earthquake Field Investigation Team*.

World Bank (2017), *World Bank Annual Report 2017 (English)*. Washington, D.C. World Bank Group. <http://documents.worldbank.org/curated/en/143021506909711004/World-Bank-Annual-Report-2017>.